Hindawi
Journal of Chemistry
Volume 2024, Article ID 1984821, 13 pages
https://doi.org/10.1155/2024/1984821

Research Article

Removal of Heavy Metal Ions (Pb^{2+}, Co^{2+}, and Cd^{2+}) by Activated Carbon from Cypress Fruit: An Investigation of Kinetics, Thermodynamics, and Isotherms

Alaa M. Al-Ma'abreh, Dareen A. Hmedat, Gada Edris, and Mariam A. Hamed

Department of Chemistry, Faculty of Science, Isra University, P.O. Box 22, Amman 11622, Jordan

Correspondence should be addressed to Alaa M. Al-Ma'abreh; alaa.almaabreh@iu.edu.jo

Received 30 October 2023; Revised 5 April 2024; Accepted 10 April 2024; Published 25 April 2024

Academic Editor: Liviu Mitu

In this study, activated carbon cloth (ACC) derived from cypress fruit was employed to investigate the adsorption of Pb^{2+}, Cd^{2+}, and Co^{2+} from synthetic aqueous systems. The correlation between adsorption features (pH, adsorbent dosage, temperature, initial ion concentration, and contact time) and adsorbent removal efficiency was investigated. Analysis by FT-IR, SEM, and EDS was employed to confirm the adsorption of metal ions onto the ACC. Results revealed the best adsorption efficiencies for heavy metal ions were attained at pH = 7, 11, 6; the adsorbent dosage of 0.06, 0.08, and 0.04 g for Pb^{2+}, Cd^{2+}, and Co^{2+}, respectively; the ion initial concentration of 50 mg·L^{-1} for Pb^{2+} and 70 mg·L^{-1} for both Co^{2+} and Cd^{2+}; and contact time of 90 minutes for both Pb^{2+} and Co^{2+} and 120 minutes for Cd^{2+}. Kinetic studies exposed the second-order adsorption of all aforementioned heavy metal ions. Additionally, the equilibrium data were fitted by Langmuir and Freundlich's isotherms, while the former performed better than the latter. The maximum adsorption capacity values for Pb^{2+}, Co^{2+}, and Cd^{2+} were attained to 81.87, 55.30, and 117.3 mg·g^{-1}, respectively. Considering the thermodynamic data, the studied processes were exothermic and spontaneous.

1. Introduction

Water pollution is a global environmental challenge that continues to pose significant threats to the well-being of both ecosystems and human populations. As one of the most vital resources on our planet, water serves as a lifeline for all living organisms, sustaining biodiversity, agriculture, industry, and domestic needs [1]. However, human activities, industrialization, agricultural practices, and improper waste disposal have led to the contamination of water bodies with various pollutants. These contaminants include a broad variety of materials that end up in rivers, lakes, seas, and groundwater sources, such as heavy metals, hazardous compounds, fertilizers, and microplastics [2]. The effects of water pollution are extensive, leading to the deterioration of aquatic environments, a decline in biodiversity, and the threat to many species. Furthermore, drinking tainted water puts one's health in danger for both acute and chronic illnesses. Since the level of water pollution is still rising, strong scientific research, environmentally friendly management techniques, and cooperative efforts at the local, national, and international levels are all needed to address this situation [3]. An urgent environmental worry nowadays is heavy metal pollution, which is brought on by the discharge of hazardous elements like lead (Pb), cobalt (Co), chromium (Cr), mercury (Hg), and cadmium (Cd) into the environment. Because they are the result of several anthropogenic activities, these heavy metals are extremely dangerous to natural systems and human health. It is well known that hazardous elements may bioaccumulate in organisms and be persistent in the environment. This can have detrimental consequences on human organs, such as the kidneys, liver, and nervous system. Furthermore, the imbalance of an ecosystem is upset by heavy metal contamination, which hurts plant growth, soil fertility, and aquatic life. Providing efficient mitigation solutions requires an

understanding of the origins, distribution, and mechanisms of heavy metal contamination [4]. The development of operative and competent technologies for the removal of heavy metal is serious as the issue of heavy metal-induced water contamination arises. Adsorption is one of the most promising and well-studied strategies for removing heavy metals from water [5]. Adsorption is constructed on the interaction of an adsorbent surface with the heavy metal ions existing in the water, which causes the ions to be engaged and removed [6]. This study focused on the removal of Pb^{2+}, Co^{2+}, and Cd^{2+} because they are widely recognized as environmental pollutants with significant implications for human health and ecosystems. Therefore, they have a prevalence and potential impact on water quality. These ions are also known to pose serious health risks even at low concentrations. Child neurotoxicity from Pb^{2+} is well known. Exposure to cobalt ions leads to respiratory and cardiovascular concerns, whereas exposure to cadmium ions leads to kidney damage and other health complications. It is required to investigate these metals to realize and lower their potential adverse health effects. Cypress fruit was preferred as an adsorbent in this study because of its availability and approachability in the region and due to the exhibit of distinctive features that strengthen its adsorption capacity. The cypress fruit-based activated carbon is characterized by its porous structure, which grants it a significant surface area and enhances its effectiveness in arresting pollutants. Moreover, the adsorption effectiveness of cypress fruit is prompted by its intrinsic chemical composition, which is in turn influenced by the local climate and soil conditions. The objective of this study is to evaluate the potential of employing cypress fruit-based activated carbon as an adsorbent for removing Pb^{2+}, Co^{2+}, and Cd^{2+} from water. This study also focuses on optimizing the conditions for efficient adsorption, studying features, such as adsorbent dosage, pH, agitation time, and initial metal ion concentration. By achieving high metal removal efficiency via adsorption onto cypress fruit-based activated carbon, this research intends to improve the remediation of water, reduce environmental contamination, and promote sustainable water treatment.

2. Materials and Methods

2.1. Chemicals. Lead (II) nitrate, cobalt (II) nitrate hexahydrate, and cadmium nitrate were purchased from Sigma-Aldrich. Sodium hydroxide and hydrochloric acid were obtained from Floka. Double-distilled water was used for the preparation of all solutions.

2.2. Preparation of Solutions. 1000 ppm stock solutions of $Pb(NO_3)_2$, $Co(NO_3)_2{\cdot}6H_2O$, and $Cd(NO_3)_2$ were prepared in double-distilled water in three separate 100-mL volumetric flasks. Thereafter, the stock solutions were diluted with distilled water to the desired concentrations. A solution mixture of the three metal ions was prepared from the stock solutions, with prescribed concentrations of each. The pH value of the solutions was adjusted using sodium hydroxide and hydrochloric acid (0.5 M).

2.3. The Preparation and Characterization of Adsorbent. Cypress fruit was collected from the Isra University campus in Jordan. Subsequently, the cypress fruits were rinsed, dried at 80°C for 48 hours, ground, impregnated with 98% phosphoric acid, heated to 450°C, and then washed to neutralization [7]. The activated carbon cloth (ACC) that was prepared experienced a procedure involving crushing and sieving, which led to the achievement of a particle size measuring 180 μm. The functional groups at the ACC surface were assessed using Fourier transform infrared (FT-IR, TENSOR model from BRUKER). The adsorption process was confirmed using the scanning electron microscopy (SEM, Apreo 2 S LoVac) technique.

2.4. Adsorption Experiment. A solution with varying concentrations of the heavy metal ion was combined with a specific quantity of ACC and afterward agitated for a predetermined duration. The quantification of the long-term presence of the heavy metal ion was conducted utilizing an atomic absorption spectrometer. The study investigated the adsorption parameters, including the dose of activated carbon cloth (ACC), the initial concentration of the heavy metal ion, the pH of the solution, the duration of agitation, and the temperature. An experiment was performed using a mixture solution of the three metal ions at the found optimal conditions. The amount of the heavy metal ion was analyzed using a ContrAA 800 Atomic Absorption Spectrometer. Equations (1) and (2), as proposed by [8], were utilized to quantify the concentration of the heavy metal ion and calculate the percentage of removal achieved by ACC.

$$\%\ \text{Removal} = \frac{\left(C_i - C_{\text{eq}}\right)}{C_{\text{eq}}} \times 100, \tag{1}$$

$$q_e = \frac{\left(C_i - C_{\text{eq}}\right)V}{w}. \tag{2}$$

The adsorbed amount of heavy metal ions in milligrams per gram (mg/g) is expressed as q_e, and the initial concentration of heavy metal ions in milligrams per liter (mg/L) is expressed as C_i. C represents the equilibrium concentration of heavy metal ions in milligrams per liter (mg/L), V represents the volume of the solution in liters (L), and m represents the mass of the ACC in grams (g).

3. Results and Discussion

3.1. Characterization of Adsorbent

3.1.1. FT-IR. FT-IR instrument with ATR unit (TENSOR model, BRUKER, Germany) was used to analyze samples. The presence of distinct peaks in the FT-IR spectra (Figure 1) confirmed the presence of specific functional groups, which are essential for understanding their adsorption properties and potential applications. The FT-IR analysis conducted on the samples, namely, ACC adsorbent, ACC-Pb^{2+}, ACC-Co^{2+}, and ACC-Cd^{2+}, indicated the presence of several functional groups in each of them. Consequently, as shown in Table 1, the presence of heavy metal ions (Pb^{2+}, Co^{2+}, and

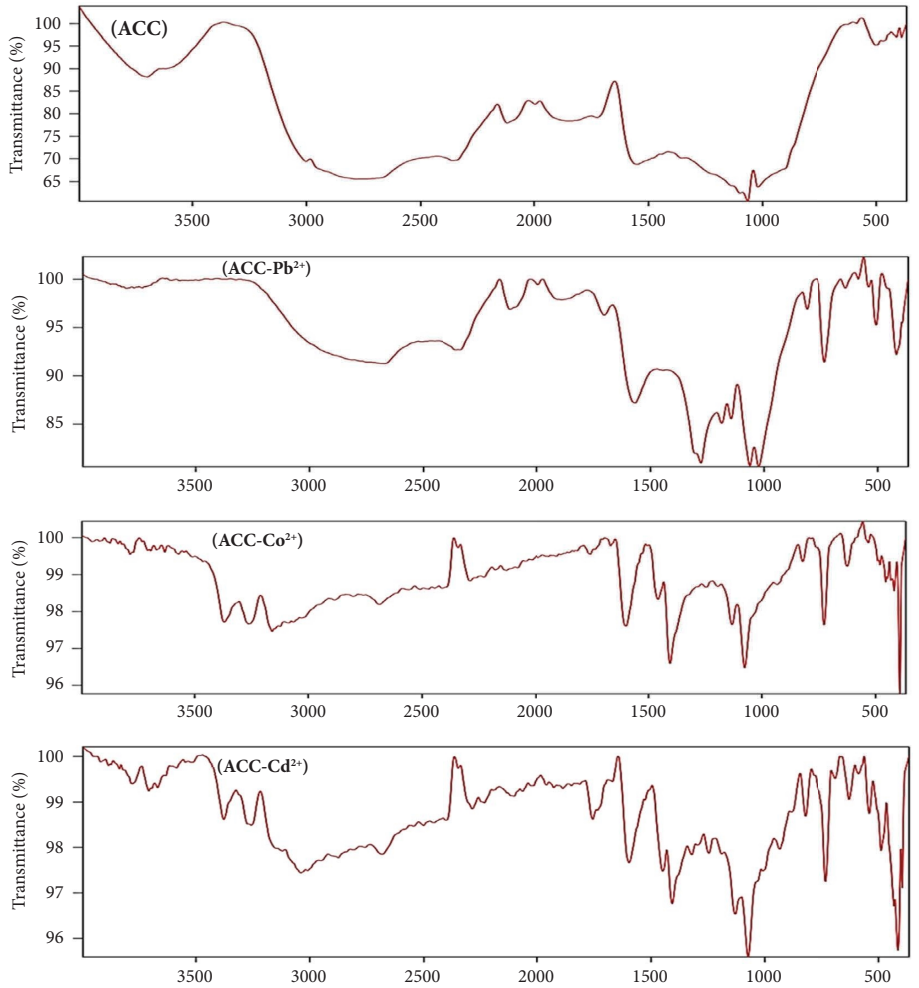

Figure 1: FT-IR analysis.

Table 1: FT-IR results of ACC, ACC-Pb^{2+}, ACC-Co^{2+}, and ACC-Cd^{2+}.

	ACC (cm^{-1})	ACC-Pb^{2+} (cm^{-1})	ACC-Co^{2+} (cm^{-1})	ACC-Cd^{2+} (cm^{-1})
O-H stretching vibration	3696	3710	3369	3378
C-H stretching	2781	2672	2687	3040
C=O stretching vibration	1723	1702	1754	1754
C-H bending	1545	1567	1456	1595
Aromatic-CH group	1021	1024	932	1074
Metal ion-O stretching	—	419, 507	433, 447, 481	316, 489

Cd^{2+}) on ACC is confirmed by the apparent variations in both absorbance and intensity. For example, there are shifts in peaks related to C-H, C=O, and O-H groups after the adsorption of heavy metal ions. The appearance of peaks in the range of 400–600 cm^{-1}, for example, at 507, 481, and 489 cm^{-1} for Pb^{2+}, Co^{2+}, and Cd^{2+}, respectively, confirmed the coordination between metal ions and oxygen atoms on the ACC surface.

3.1.2. SEM and EDS. The changes in surface characteristics of ACC adsorbent after the adsorption of the heavy metal ion (Pb^{2+}, Co^{2+}, Cd^{2+}, and Mix) confirm the adsorption process as shown in Figures 2(a)–2(e).

Scanning electron microscopy (SEM) analysis was employed to investigate the changes in the pore and surface characteristics of the ACC samples both before and after ion adsorption. According to the SEM picture depicted in Figure 2(a), it can be observed that the surface of the adsorbent material exhibits a porous structure, characterized by a significant quantity of pores distributed over its surface. This morphology renders the adsorbent material suitable for effectively removing contaminants. Additionally, the SEM micrographs presented in Figures 2(b)–2(e) present the adsorbent's surface after the profitable removal of Pb^{2+}, Co^{2+}, Cd^{2+}, and a mixture of the three ions. These micrographs reveal that the surface pores were effectively covered anticipating the adsorption of the aforementioned ions.

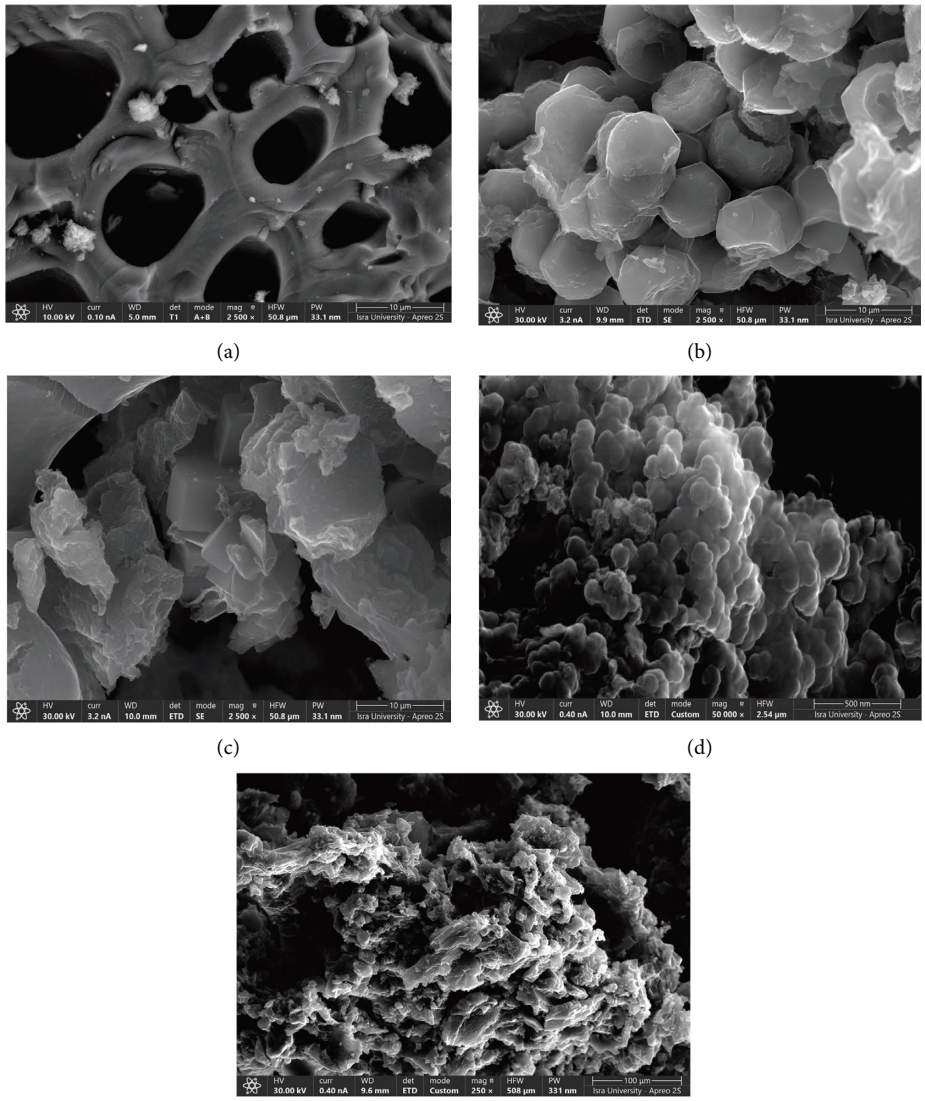

Figure 2: SEM analysis of (a) ACC, (b) ACC-Pb^{2+}, (c) ACC-Co^{2+}, (d) ACC-Cd^{2+}, and (e) ACC-Mix.

The EDS analysis findings (Figure 3) show the presence of many elements, such as carbon (C), oxygen (O), phosphorus (P), sodium (Na), and potassium (K), in the adsorbent (ACC) that was synthesized. Furthermore, after the adsorption process of Pb^{2+}, Co^{2+}, and Cd^{2+}, it is evident from the results of the EDS study that these elements were detected after adsorption. This observation signifies that the aforementioned ions were effectively adsorbed by ACC. Moreover, carbon has emerged as a prominent element within the studied samples of activated carbon. According to the data presented in Table 2, the weight percentages of Pb^{2+}, Co^{2+}, and Cd^{2+} within the activated carbon framework were found to be 5.64%, 3.39%, and 6.85%, respectively. This implies that the aforementioned ions have been affixed to the active sites of the ACC through the adsorption process. The data presented in the figures also indicate a greater affinity of the adsorbent derived from cypress fruit for the removal of cadmium ions from the aqueous solution, as compared to the other two ions.

3.2. Batch Adsorption

3.2.1. Impact of the Adsorbent Mass. The percentage of adsorption is influenced by the total amount of the adsorbent material. In the present investigation, the administered amount of ACC ranges from 0.02 to 0.1 grams, with the temperature maintained at $25.0 \pm 1^{\circ}C$. The results presented in Figure 4 demonstrate the most effective amount of ACC for the removal of Pb^{2+}, Co^{2+}, and Cd^{2+}, which have been determined to be 0.06, 0.08, and 0.04 g, respectively. There has been a notable increase in the adsorption of the aforementioned ions starting out, attributed to the presence of easily accessible active sites for adsorption. However, this adsorption decreases as the system approaches equilibrium.

3.2.2. Impact of the Ions Initial Concentration. The study investigated the influence of the initial concentration on the adsorption of the heavy metal ions aforementioned on ACC. The concentration range experienced was between 30 and

Table 2: EDS analysis of ACC before and after adsorption.

Element	Sample							
	ACC		ACC-Pb^{2+}		ACC-Co^{2+}		ACC-Cd^{2+}	
	% Weight	% Atom	% Weight	% Atom	% Weight	% Atom	% Weight	% Atom
C	67.99	76.36	64.85	74.42	72.88	80.46	67.15	78.97
O	21.14	17.83	28.66	24.69	21.52	17.84	18.63	16.45
Na	7.17	4.21	0.86	0.51	0.0	0.0	2.26	1.39
P	3.69	1.61	0.0	0.0	2.21	0.94	5.11	2.33
Pb	0.0	0.0	5.64	0.38	0.0	0.0	0.0	0.0
Co	0.0	0.0	0.0	0.0	3.39	0.76	0.0	0.0
Cd	0.0	0.0	0.0	0.0	0.0	0.0	6.85	0.86

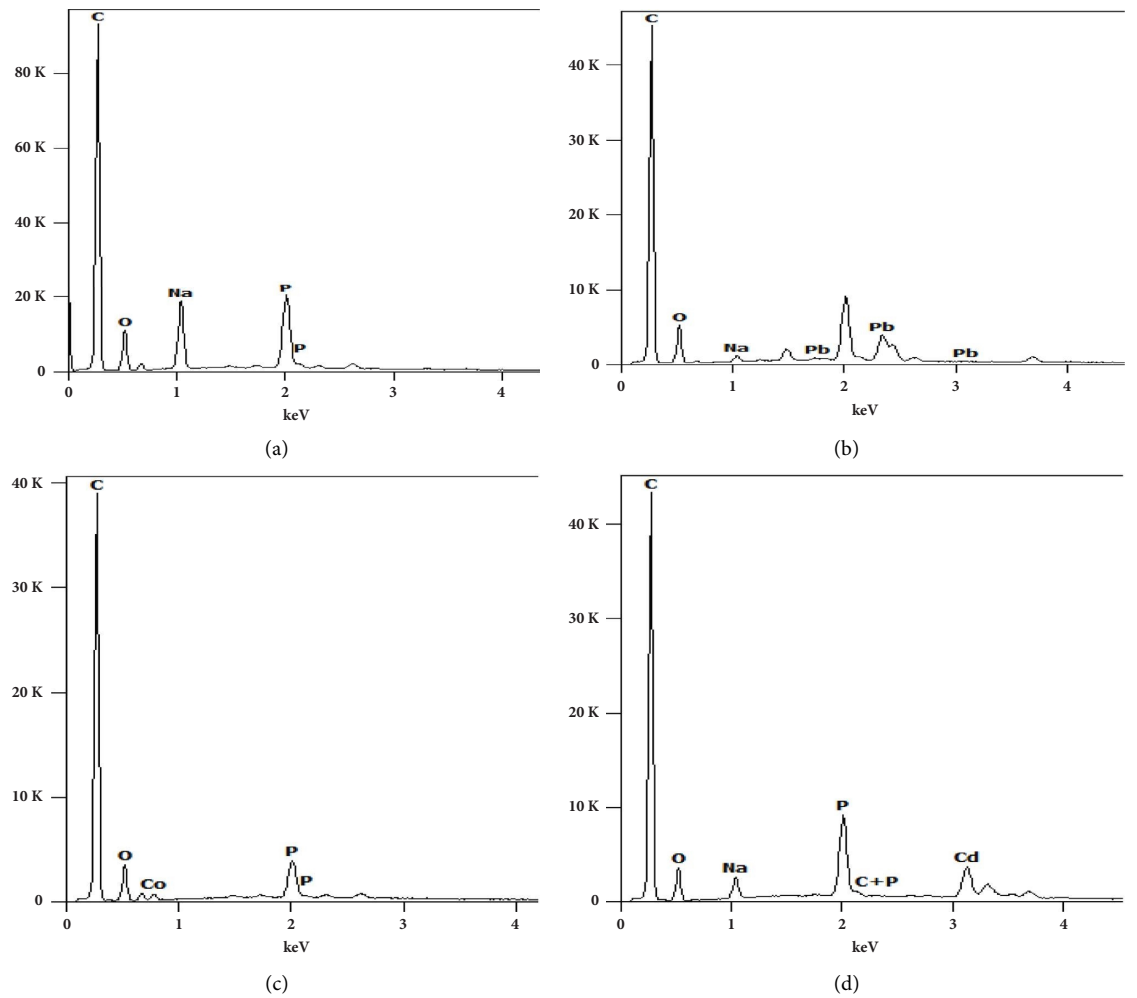

Figure 3: EDS analysis of (a) ACC, (b) ACC-Pb^{2+}, (c) ACC-Co^{2+}, and (d) ACC-Cd^{2+}.

120 mg·L^{-1} at 25 ± 1°C. Figure 5 demonstrates the influence of the initial concentration on the adsorption of heavy metal ions onto ACC. The experiment yielded ideal adsorption percentages of 96.48% for Pb^{2+}, 83.54% for Co^{2+}, and 91.21% for Cd^{2+} onto ACC samples weighing 0.06 g, 0.08 g, and 0.04 g, respectively. The optimal concentrations of Pb^{2+}, Co^{2+}, and Cd^{2+} were found to be 50, 70, and 70 mg·L^{-1}, respectively. The rise in the concentration of heavy metal ions resulted in a corresponding increase in the number of occupied sites on the surface of the ACC. Consequently, this increase in occupied sites led to a decrease in the adsorption process ended by equilibrium.

3.2.3. Impact of Adsorption Duration. The batch adsorption studies involved agitating 0.06, 0.08, and 0.04 g of ACC with 50 ml of 50 mg·L^{-1} Pb^{2+} and 70 mg·L^{-1} Co^{2+}, and Cd^{2+} at 25 ± 1°C for a time period ranging from 30 to 180 minutes. Figure 6 shows the variation in the adsorption of the

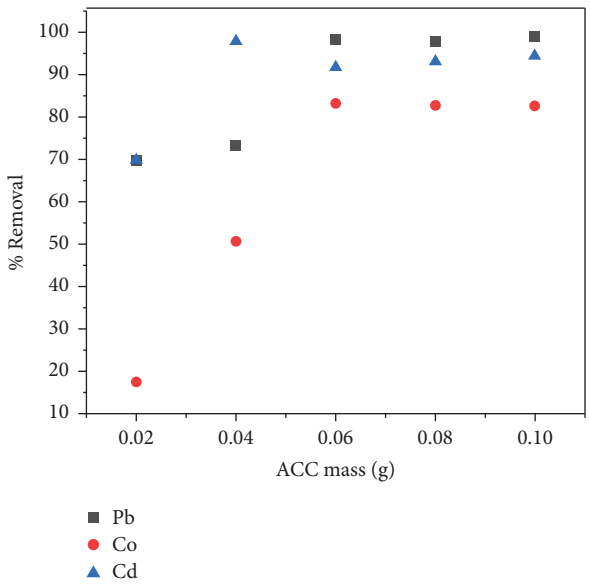

Figure 4: Impact of ACC mass on the adsorption of Pb^{2+}, Co^{2+}, and Cd^{2+}.

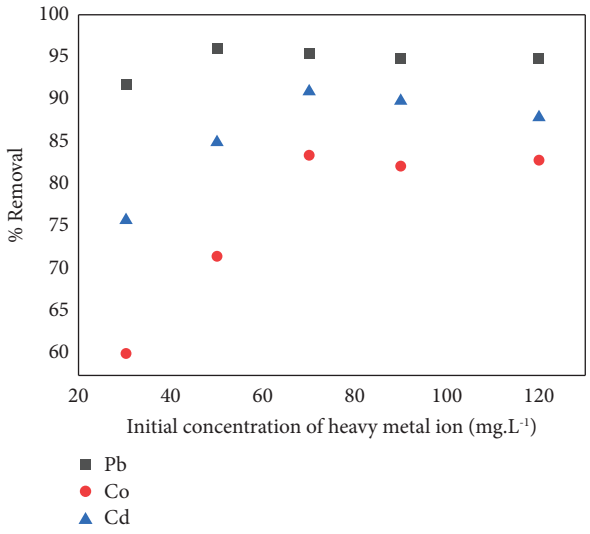

Figure 5: Impact of heavy metal initial concentration.

aforementioned ions onto the ACC as time increased. The optimal adsorption duration was 90 minutes for Pb^{2+} and Co^{2+}, and 120 minutes for Cd^{2+}.

3.2.4. Determination of pHpzc. Determining the pHpzc value is of significant importance as it provides insight into the pH level at which the surface of the adsorbent attains neutrality. The pH at the point of zero charges (pHpzc) was determined by subjecting a mixture of 0.15 g of ACC and 50.0 ml of a 0.1 M NaCl solution to agitation throughout a pH range of 2 to 12 for approximately 24 hours [7]. According to the results presented in Figure 7, it can be observed that the surface of ACC exhibits neutrality at a pH value of 7.0.

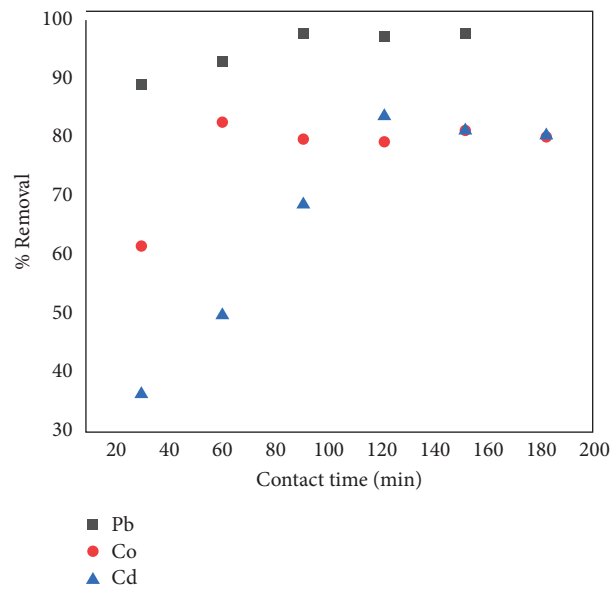

Figure 6: Impact of adsorption duration time.

3.2.5. Impact of pH. In this investigation, 50 ml of heavy metal ion solution was agitated with a predetermined amount of ACC as follows: 50.0 $mg{\cdot}L^{-1}$ Pb^{2+} with 0.06 g ACC for 90 minutes, 70 $mg{\cdot}L^{-1}$ Co^{2+} with 0.08 g ACC for 90 minutes, and 70 $mg{\cdot}L^{-1}$ Cd^{2+} with 0.04 g ACC for 120 minutes. These adsorption processes were conducted at a temperature of $25 \pm 1^{\circ}C$ and a pH ranging from 3 to 11. Based on the results shown in Figure 8, it can be concluded that the pH level does not exert any significant influence on the adsorption process of Pb^{2+} onto ACC. The utilization of a neutral solution is considered optimal for the adsorption of both Co^{2+} and Cd^{2+} ions.

3.2.6. Adsorption of Metal Ions Mixture. A batch adsorption experiment was conducted by shaking 0.08 g of ACC with a 50 ml solution consisting of 50 Pb^{2+}, 70 $mg{\cdot}L^{-1}$ of Co^{2+}, and Cd^{2+} for 100 minutes. The findings indicated that the ACC exhibited a higher affinity toward Pb^{2+} compared to Co^{2+} and Cd^{2+}, with percentages of 96.5%, 89.7%, and 65%, respectively.

3.3. Kinetic and Mechanism. Linear and nonlinear kinetics models, performing pseudo-first-order (PFO), pseudo-second-order (PSO), and intraparticle diffusion (IPD), were hired to investigate the kinetics of the adsorption process of Pb^{2+}, Co^{2+}, and Cd^{2+} onto the surface of ACC. Equations 3 to 6 were utilized to signify the adsorption of the aforementioned heavy metal ions onto ACC.

$$\log(q_e - q_t) = \log(q_e) - \left(\frac{k_1}{2.303}\right)t, \tag{3}$$

$$q_t = q_e\left(1 - e^{-k_1 t}\right)t, \tag{4}$$

$$\frac{t}{q_t} = \frac{1}{k_2 q_e^2} - \frac{1}{q_e}t, \tag{5}$$

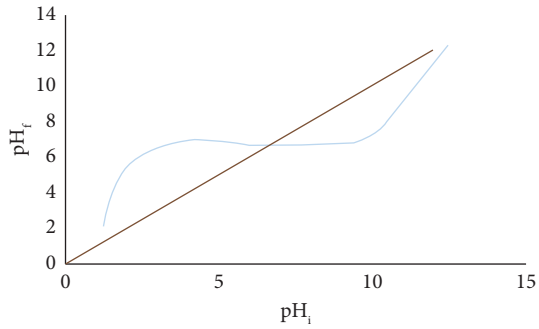

Figure 7: pH_{pzc} for ACC.

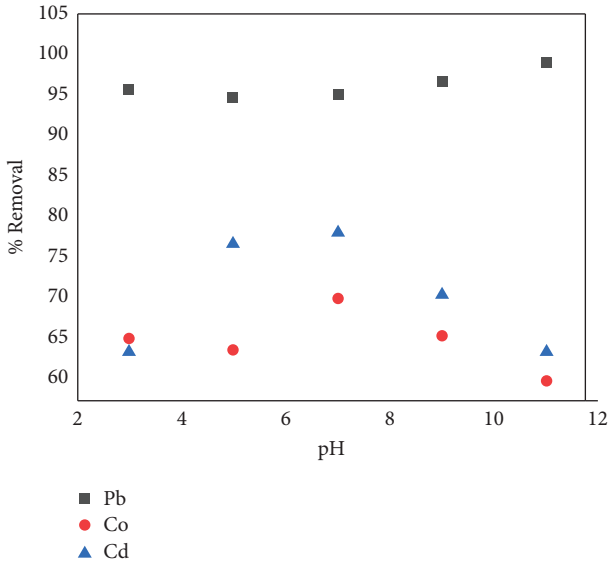

Figure 8: Impact of pH.

$$q_t = \frac{q_e^2 k_2 t}{q_e k_2 t + 1}, \tag{6}$$

where q_e is the amount of metal ion per unit mass of ACC ($mg \cdot g^{-1}$) at equilibrium, q_t is the amount of metal ion per unit mass of ACC at time t ($mg \cdot g^{-1}$) at equilibrium, and k_1 and k_2 are the rate constant in min^{-1} and $g \cdot mg^{-1} \cdot min^{-1}$, respectively.

The results depicted in Figures 9 and 10 demonstrate conclusively that the pseudo-second-order model affords the most accurate representation of the kinetics associated with the adsorption of the aforementioned ions onto ACC. The results of the nonlinear models are consistent with those of the linear models. Those results are succinctly presented in Table 3.

The mechanism of the heavy metal ions adsorption onto ACC was demonstrated using intraparticle diffusion, as shown in equations (9) and (10) [9]:

$$q_t = K_{id} t^{1/2} + C, \tag{7}$$

$$q_t = K_{id} t^{1/2}, \tag{8}$$

where q_t is the heavy metal ion amount ($mg \cdot g^{-1}$), K_{id} is the rate constant ($mg \cdot g^{-1} \cdot min^{-0.5}$), and $t^{1/2}$ is the square root of time ($min^{0.5}$). According to the intraparticle diffusion model, it can be inferred that when the intercept C equals zero, the sole factor limiting the rate of the process is the intraparticle diffusion. When the constant C is greater than zero, the relevance of surface adsorption increases. Figure 11 proves that surface adsorption, not intraparticle diffusion, is the rate-limiting step in the adsorption process for Pb^{2+}, while the two steps control the adsorption processes of both Co^{2+} and Cd^{2+}.

Table 3 summarizes the R^2 and constant values for all kinetics models.

3.4. Adsorption Isotherms. Adsorption isotherm models are usually employed to examine the correlation between the adsorbent and the adsorbate, as well as to ascertain the nature of the adsorption process, whether it is physical or chemical in nature. The adsorption mechanism of the metal ions (Pb^{2+}, Co^{2+}, and Cd^{2+}) on ACC was investigated using Langmuir (equations (9) and (10)), Freundlich (equations (11) and (12)), Dubinin-Radushkevich (D-R) (equations (13) and (14)), and Temkin (equations (15) and (16)) isothermal models [10].

$$\frac{C_e}{q_e} = \frac{1}{k_L q_m} + \frac{C_e}{q_m}, \tag{9}$$

$$q_e = \frac{k_L q_m C_e}{(1 + k_L C_e)}, \tag{10}$$

where q_e is the equilibrium magnitude of the metal ion ($mg \cdot g^{-1}$), C_e is the equilibrium concentration of the metal ion ($mg \cdot L^{-1}$), K_L is the constant of Langmuir isotherm that usually in use to determine adsorbate association to the adsorbent surface, and q_m is the adsorption capacity ($mg \cdot g^{-1}$).

$$\log q_e = \log K_f + \frac{1}{n} \log C_e, \tag{11}$$

$$q_e = K_F C_e^{\,1/n}. \tag{12}$$

The constant K_f represents the Freundlich isotherm constant, measured in units of $mg \cdot g^{-1}$. Meanwhile, the parameter n denotes the adsorption intensity.

$$q_e = B \ln A + B \ln C_e, \tag{13}$$

$$q_e = B \ln AC_e. \tag{14}$$

The binding constant A is measured in units of g^{-1} when the system is at equilibrium, while the adsorption heat is consistently related to the variable B.

$$\ln q_e = \ln Q_D - B_D \varepsilon^2, \tag{15}$$

$$q_e = q_m e^{-B_D \varepsilon^2}. \tag{16}$$

The maximum theoretical capacity (Q_D) is expressed in units of $mol \cdot g^{-1}$, whereas the D-R constant (B_D) is measured in units of $mol^2 \cdot kJ^{-2}$. The Polanyi potential (ε) in the D-R

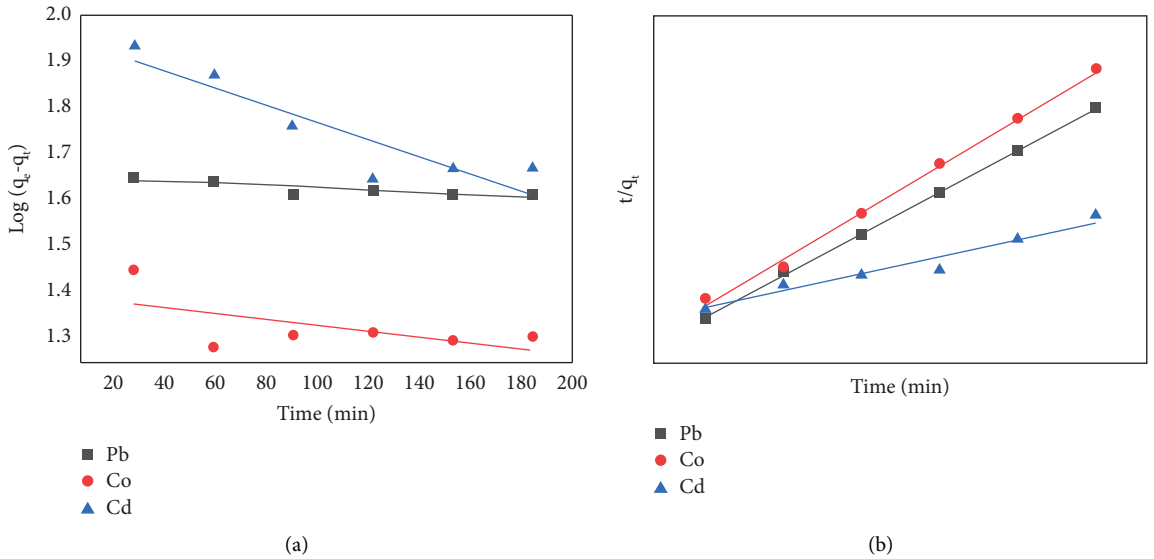

Figure 9: Linear kinetic studies of the uptake of metal ions by ACC (a) PFO and (b) PSO.

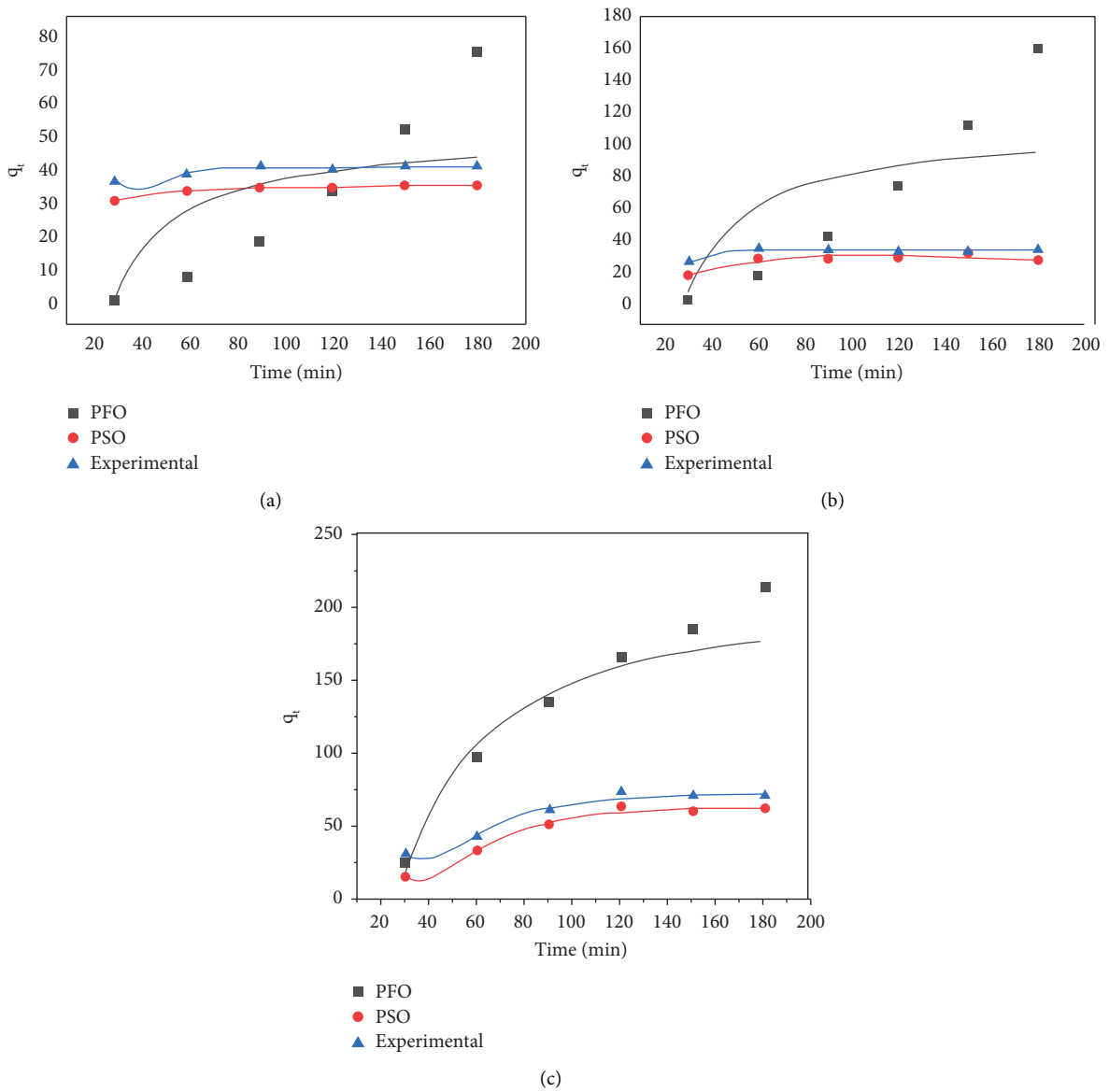

Figure 10: Nonlinear kinetics of the adsorption of (a) Pb^{2+}, (b) Co^{2+}, and (c) Cd^{2+} on ACC.

Table 3: Results of kinetics studies for the Pb^{2+}, Co^{2+}, and Cd^{2+} adsorption onto ACC.

Kinetic model		Linear models	
		R^2	Related constants
PFO	Pb^{2+}	0.7597	$K_1 = 4.61 \times 10^{-4}$ (min^{-1})
	Co^{2+}	0.3481	$K_1 = 1.38 \times 10^{-3}$ (min^{-1})
	Cd^{2+}	0.8222	$K_1 = 4.38 \times 10^{-3}$ (min^{-1})
PSO	Pb^{2+}	0.9966	$K_2 = 4.65 \times 10^{-3}$ ($g \cdot mg^{-1} \cdot min^{-1}$)
	Co^{2+}	0.9998	$K_2 = 6.27 \times 10^{-3}$ ($g \cdot mg^{-1} \cdot min^{-1}$)
	Cd^{2+}	0.9543	$K_2 = 1.52 \times 10^{-4}$ ($g \cdot mg^{-1} \cdot min^{-1}$)
IPD	Pb^{2+}	0.8430	$K_{id} = 0.4687$ ($mg \cdot g^{-1} \cdot min^{-0.5}$)
	Co^{2+}	0.4622	$K_{id} = 0.7779$ ($mg \cdot g^{-1} \cdot min^{-0.5}$)
	Cd^{2+}	0.8873	$K_{id} = 5.4366$ ($mg \cdot g^{-1} \cdot min^{-0.5}$)

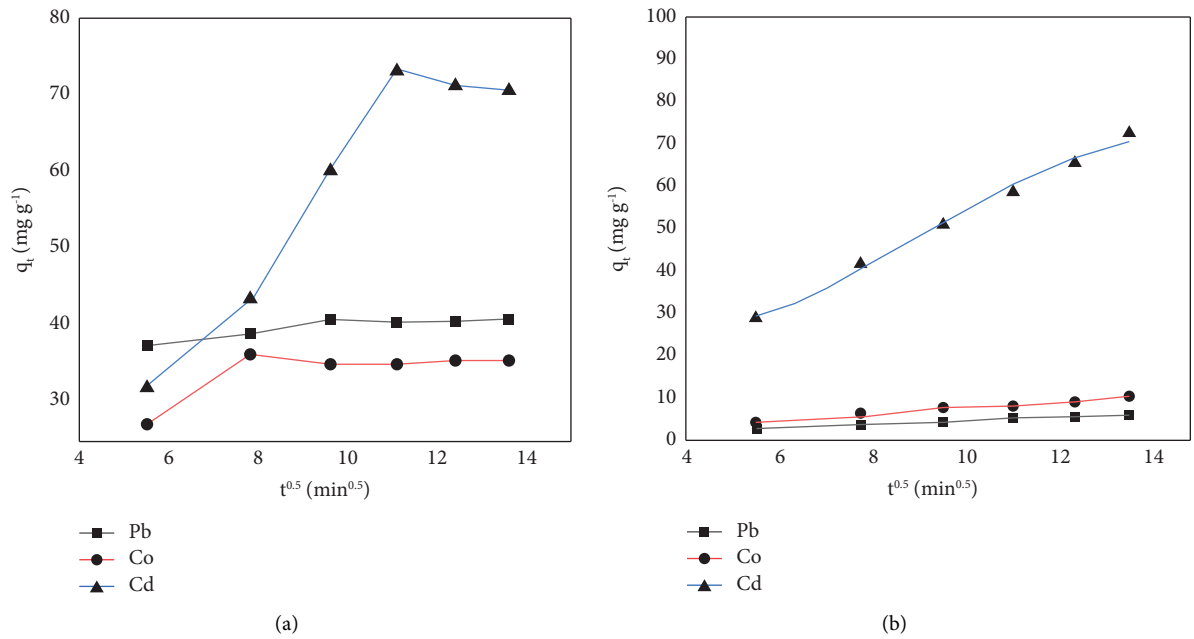

Figure 11: (a) Linear and (b) nonlinear intraparticle model for the adsorption of the heavy metal ions (Pb^{2+}, Co^{2+}, and Cd^{2+}) on ACC.

isotherm can be determined by employing equation (17), whereas the mean energy of adsorption (in $kJ \cdot mol^{-1}$) can be calculated using equation (18) as follows:

$$\varepsilon = \mathrm{RTln}\left(1 + \frac{1}{C_e}\right), \tag{17}$$

$$E = \frac{1}{\sqrt{2B_D}}. \tag{18}$$

Figures 12(a)–12(d) show the linear form of the four isotherms. Table 4 summarizes plot-based correlation coefficients (R^2), dimensional components, and constants. The Langmuir isotherm adequately assessed ACC metal ion removal, as shown by the high R^2 values (0.9971, 0.9926, and 0.9951 for Pb^{2+}, Co^{2+}, and Cd^{2+}, respectively) indicating ACC surface uniformity and adsorption site homogeneity. Based on D-R isotherm calculations, Pb^{2+}, Co^{2+}, and Cd^{2+} have energy values of 25, 7.538, and 8.452 $kJ \cdot mol^{-1}$, respectively. Co^{2+} is physically removed, whereas Pb^{2+} and Cd^{2+} are chemically removed. The negative Temkin constant values B (−6.04, −14.0, and −25.68 for Pb^{2+}, Co^{2+}, and Cd^{2+}, respectively) indicate a significant interaction between the metal ion and the ACC adsorbent [11].

3.5. Thermodynamics. Thermodynamic studies were performed under controlled conditions at temperatures of 298 ± 1 K, 308 ± 1 K, and 318 ± 1 K, with a consistent agitation duration of 1.0 hour. Thermodynamic parameters, namely, ΔG°, ΔH°, and ΔS°, were computed to assess the effectiveness of metal ion removal by ACC. These results are presented in Table 5. The enthalpy change (ΔH°) and entropy change (ΔS°) associated with the removal of metal ions were determined by analyzing the slope and intercept of the plot of the natural logarithm of the equilibrium constant ($\ln K_L$) against the reciprocal of temperature (1/T), as described in equation (19). The calculation of the standard Gibbs free energy, ΔG°, was performed using equation (20) as follows:

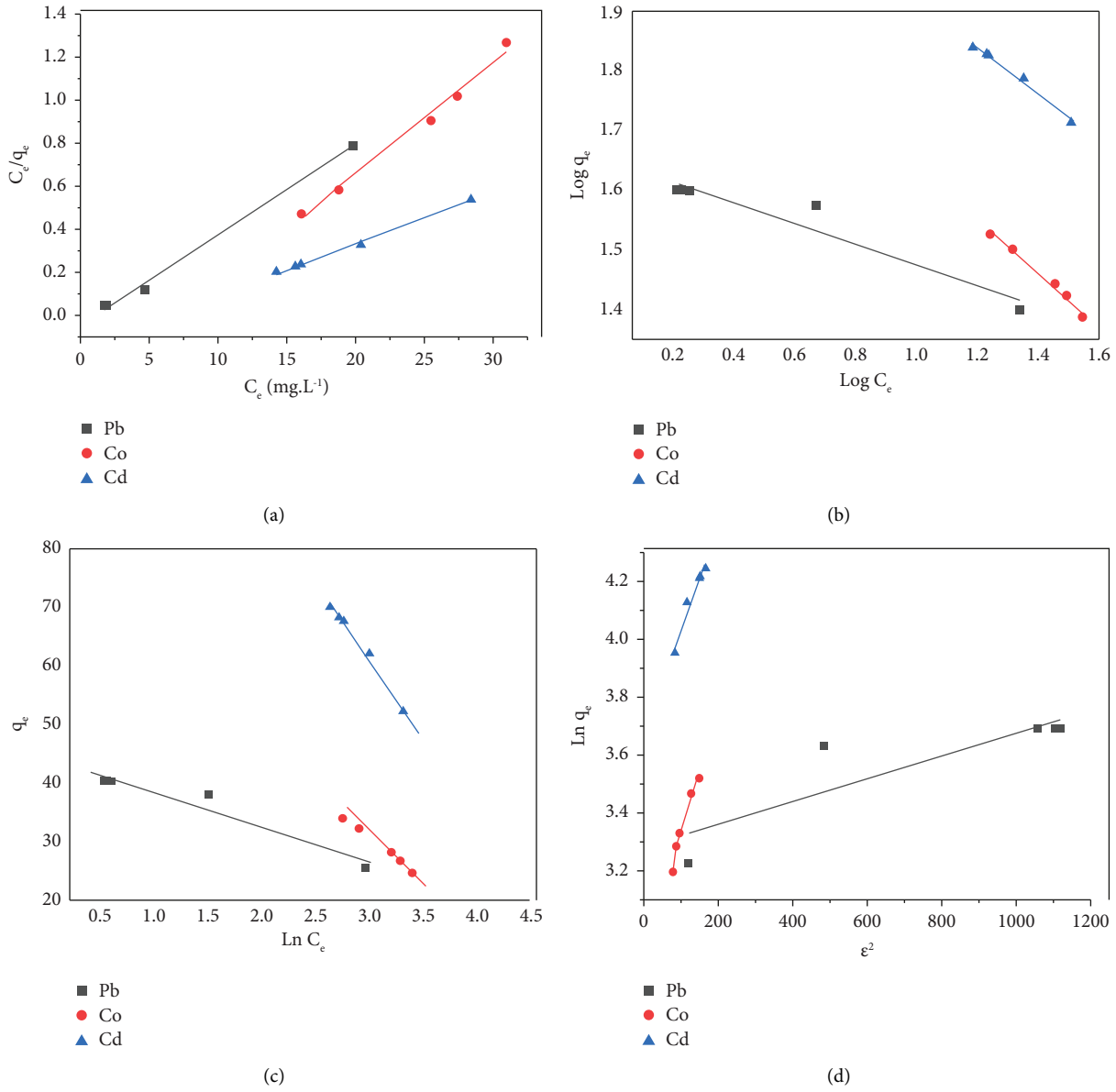

Figure 12: The linear isotherms of (a) Langmuir, (b) Freundlich, (c) Temkin, and (d) D-R of Pb^{2+}, Co^{2+}, and Cd^{2+} removal by ACC.

Table 4: Isotherm model constants.

Isotherm	Related isotherm constants	Metal ion		
		Pb^{2+}	Co^{2+}	Cd^{2+}
Langmuir	R_L^2	0.9971	0.9926	0.9951
	K_L	1.0725	0.1356	0.1624
	q_m, mg·g^{-1}	84.15	79.16	61.32
Freundlich	R_F^2	0.9278	0.9851	0.9847
	K_F, mg·g^{-1}	5.26	8.27	10.37
	n	5.0	2.0	2.0
D-R	R^2	0.7726	0.9621	0.9564
	B_D, mol^2·kJ^{-2}	4.0×10^{-4}	4.40×10^{-3}	3.50×10^{-3}
	E, kJ·mol^{-1}	25.00	7.54	8.45
Temkin	R^2	0.9418	0.9935	0.9922
	B	−6.037	−14.00	−25.68
	A	4.60×10^{-8}	6.27×10^{-6}	4.04×10^{-6}

Table 5: Thermodynamic parameters of metal ion removal by ACC.

Metal ion	T (K)	Thermodynamic parameters		
		ΔG° (kJ mol^{-1})	ΔH° (kJ mol^{-1})	ΔS° (kJ K^{-1}·mol^{-1})
Pb	298	12.45	22.24	33.22
	308	12.01		
	318	11.79		
Co	298	15.81	21.08	17.76
	308	15.56		
	318	15.46		
Cd	298	17.68	34.26	56.12
	308	16.66		
	318	16.57		

$$\ln(K_L) = \frac{\Delta S^o}{R} - \frac{\Delta H^o}{T}\left(\frac{1}{T}\right), \quad (19)$$

$$\Delta G^o = -\mathrm{RT}\ln(K_L), \quad (20)$$

where K_L is dimensionless and corresponds to the adsorption equilibrium constant according to the best-fitted model, and R is the universal constant of ideal gases (8.314 J·K^{-1}·mol^{-1}). The +ve obtained value of ΔG° (11.81, 11.85, and 11.88 kJ·mol^{-1}) indicates the nonspontaneity of the metal ion adsorption by ACC. The +ve acquired value of ΔH° (22.24, 21.08, and 34.26 kJ·mol^{-1} for Pb^{2+}, Co^{2+}, and Cd^{2+}, respectively) indicates the endothermic nature of the aforementioned ions [12]. The +ve value of ΔS° indicates adsorbate/adsorbent interface anomaly and adsorbent affinity [13].

3.6. Synthetic Sample. Three synthetic samples were prepared by dissolving different kinds of heavy metal salts and other chemicals in tap water and agitated with 0.07 g of ACC under the optimum conditions for each ion. Figure 13 proves the efficacy of ACC in the adsorption of metal ions Pb^{2+}, Co^{2+}, and Cd^{2+}.

4. Adsorption/Desorption

Based on previous studies, it was found that 0.1 M hydrochloric acid is an appropriate choice for the recovery investigation. Metal ions of Pb^{2+}, Co^{2+}, and Cd^{2+} were eluted from ACC and subjected to atomic absorption analysis. The percentage of recovery was computed using the following equation [14]:

$$\%\,\mathrm{Recovery} = \frac{C_{de}}{C_{ad}} \times 100, \quad (21)$$

where C_{de} is the desorbed concentration of the metal ions, and C_{ad} is the adsorbed concentration of the metal ions. Figure 14 confirms that after five cycles, the recovery of metal ions declined from 89.29% to 73.14% for Pb^{2+}, from 66.49% to 43.77% for Co^{2+}, and from 64.94 to 51.36 for Cd^{2+} signaling the ability of ACC to be reused several times.

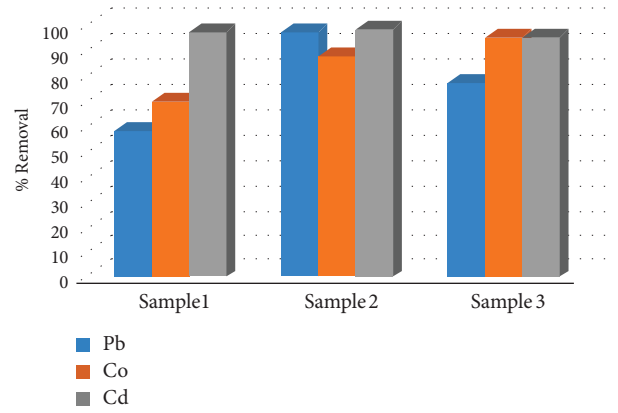

Figure 13: The adsorption of metal ions Pb^{2+}, Co^{2+}, and Cd^{2+} on ACC for synthetic samples.

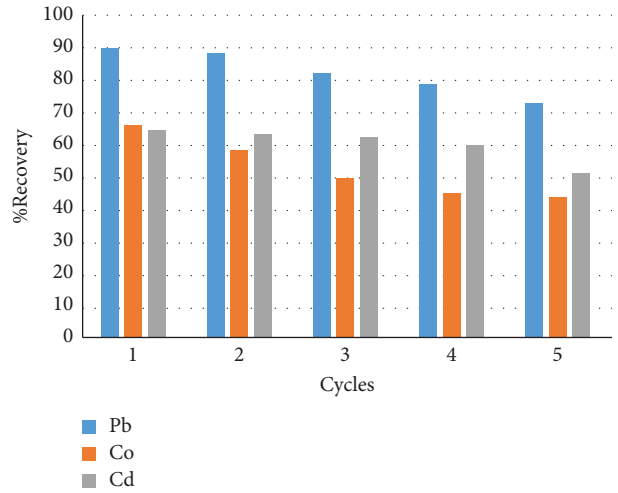

Figure 14: Regeneration of OAC adsorbent.

Table 6: Comparison of heavy metal ions adsorption onto ACC with other reported adsorbents.

Adsorbent	q_{max} (mg/g)
Olive branches AC [15]	41.32 Pb^{2+}, 38.17 Cd^{2+}
Tea and coffee powder [16]	244 Co^{2+}
Orange peel powder [17]	11.48 Co^{2+}
Orange peel [18]	85.7 Cd^{2+}
Onion outer layer [19]	60.02 Cd^{2+}
Lettuce leaves [20]	68.2 Pb^{2+}
Cypress fruit AC (present study)	84.15 Pb^{2+}, 79.16 Co^{2+}, 61.32 Cd^{2+}

5. Comparison with Other Activated Carbon

The maximum heavy metal ions removal capacities of ACC were compared to other activated carbon adsorbent (Table 6). The comparison shows that ACO has an adsorption capacity of 97.91 mg·g^{-1} near to many of the other reported adsorbents.

6. Conclusion

The current study validates the efficient removal of heavy metal ions (Pb^{2+}, Co^{2+}, and Cd^{2+}) from aqueous solutions and synthetic samples by the employment of activated carbon prepared from cypress fruit (ACC) through batch adsorption. The results of the experiments have definitively demonstrated the optimal parameters that are most suitable for attaining the highest possible removal of heavy metal ions (Pb^{2+}, Co^{2+}, and Cd^{2+}) using ACC. It is clear from the experimental data that the best conditions for ACC to remove Pb^{2+}, Co^{2+}, and Cd^{2+} are 90 minutes of shaking for Pb^{2+} and Co^{2+}, 120 minutes for Cd^{2+}, and 0.06, 0.08, and 0.04 g of ACC for Pb^{2+}, Co^{2+}, and Cd^{2+}, respectively. Additionally, the results revealed that Pb^{2+} is best removed in a neutral solution, but a basic solution works better for Co^{2+} and acidic solutions work better for Cd^{2+}. ACC showed a higher affinity toward Pb^{2+} compared to Co^{2+} and Cd^{2+}. Kinetics and isothermal analyses have shown that the adsorption of heavy metal ions by ACC closely matches both the Freundlich isothermal model and the pseudo-second-order kinetic model. Moreover, the thermodynamic analysis demonstrated that ACC uses an endothermic, non-spontaneous method to remove heavy metal ions from the environment. The effectiveness of an ACC would decrease after five cycles, but it would yet be functional.

Data Availability

The data that support the findings of this study are included within the article.

Additional Points

Statement of Novelty. The novelty of this research lies in the comprehensive investigation of kinetics, thermodynamics, and isotherms, providing a holistic understanding of the adsorption process. The unique source of activated carbon from cypress fruit sets this study apart, offering a sustainable and environmentally friendly solution for heavy metal removal. *Statement of Industrial Relevance*. The findings of this research bear significant industrial relevance by presenting an efficient and eco-friendly method for removing hazardous heavy metal ions from industrial effluents. The use of activated carbon from cypress fruit not only addresses environmental concerns but also offers a sustainable alternative for industries seeking effective water treatment solutions.

Disclosure

The authors confirm that this work is original and has not been published elsewhere nor is it currently under consideration for publication elsewhere.

Conflicts of Interest

The authors declare that they have no conflicts of interest.

Authors' Contributions

All authors contributed to the study conception and design and were responsible for material preparation, data collection, and analysis. Alaa Mahmoud Al-Ma'abreh wrote the first draft of the manuscript, and all authors commented on previous versions of the manuscript and read and approved the final manuscript.

Acknowledgments

The authors would like to express their appreciation to Isra University Innovation Center (IUIC) for the vital role in testing the samples. The state-of-the-art infrastructure at IUIC significantly contributed to the accuracy of our findings, and we are grateful for their commitment and professionalism. This research was funded by Isra University (grant no. 8-38/2020/2021).

References

[1] S. M. Bassem, "Water pollution and aquatic biodiversity," *Biodiversity International Journal*, vol. 4, no. 1, pp. 10–16, 2020.

[2] N. S. Akhtar, M. I. Syakir Ishak, S. A. Bhawani, and K. Umar, "Various natural and anthropogenic factors responsible for water quality degradation: a review," *Water*, vol. 13, no. 19, p. 2660, 2021.

[3] V. A. Tzanakakis, N. V. Paranychianakis, and A. N. Angelakis, "Water supply and water scarcity," *Water*, vol. 12, no. 9, p. 2347, 2020.

[4] S. Mitra, A. J. Chakraborty, A. M. Tareq et al., "Impact of heavy metals on the environment and human health: novel therapeutic insights to counter the toxicity," *Science*, vol. 34, no. 3, Article ID 101865, 2022.

[5] G. Lin, B. Zeng, J. Li et al., "A systematic review of metal organic frameworks materials for heavy metal removal: synthesis, applications and mechanism," *Chemical Engineering Journal*, vol. 460, Article ID 141710, 2023.

[6] J. Li, X. Dong, X. Liu et al., "Comparative study on the adsorption characteristics of heavy metal ions by activated carbon and selected natural adsorbents," *Sustainability*, vol. 14, no. 23, Article ID 15579, 2022.

[7] A. M. Al-Ma'abreh, G. edris, and M. K. Haddad, "Sonicating for the uptake of paracetamol from solution by activated carbon from oak: kinetics, thermodynamics, and isotherms," *Adsorption Science and Technology*, vol. 2023, p. 2023, 2023.

[8] Y. Önal, C. Akmil-Başar, and Ç Sarıcı-Özdemir, "Elucidation of the naproxen sodium adsorption onto activated carbon prepared from waste apricot: kinetic, equilibrium and thermodynamic characterization," *Journal of Hazardous Materials*, vol. 148, no. 3, pp. 727–734, 2007.

[9] R. Lafi, I. Montasser, and A. Hafiane, "Adsorption of Congo red dye from aqueous solutions by prepared activated carbon with oxygen-containing functional groups and its regeneration," *Adsorption Science and Technology*, vol. 37, no. 1-2, pp. 160–181, 2018.

[10] A. M. Al-Ma'abreh, M. AlKhabbas, G. Edris et al., "Exploring the kinetics, thermodynamics, and isotherms of sodium naproxen uptake by oak-based activated carbon with ultrasonic enhancement," *Desalination and Water Treatment*, vol. 300, pp. 75–83, 2023.

[11] E. Malkoc and Y. Nuhoglu, "Fixed bed studies for the sorption of chromium(VI) onto tea factory waste," *Chemical Engineering Science*, vol. 61, no. 13, pp. 4363–4372, 2006.

[12] G. R. Mahdavinia, F. Bazmizeynabad, and B. Seyyedi, "*kappa*-Carrageenan beads as new adsorbent to remove crystal violet dye from water: adsorption kinetics and isotherm-carrageenan beads as new adsorbent to remove crystal violet dye from water: adsorption kinetics and isotherm," *Desalination and Water Treatment*, vol. 53, no. 9, pp. 2529–2539, 2015.

[13] Q. Li, Q. Y. Yue, Y. Su, B. Y. Gao, and H. J. Sun, "Equilibrium, thermodynamics and process design to minimize adsorbent amount for the adsorption of acid dyes onto cationic polymer-loaded bentonite," *Chemical Engineering Journal*, vol. 158, no. 3, pp. 489–497, 2010.

[14] P. V. Nidheesh, R. Gandhimathi, S. Ramesh, and T. Singh, "Adsorption and desorption characteristics of crystal violet in bottom ash column," *Journal of Urban and Environmental Engineering*, vol. 6, no. 1, pp. 18–29, 2012.

[15] A. M. Alkherraz, "Removal of Pb(II), Zn(II), Cu(II) and Cd(II) from aqueous solutions by adsorption onto olive branches activated carbon: equilibrium and thermodynamic studies," *Chemistry International*, vol. 6, no. 1, pp. 11–20, 2020.

[16] K. M. Elsherif, "ADSORPTION OF Co(II) IONS FROM AQUEOUS SOLUTION ONTO TEA AND COFFEE POWDER: equilibrium and kinetic studies," *Journal of Fundamental and Applied Sciences*, vol. 11, no. 1, pp. 65–85, 2019.

[17] K. E.-A. Elsherif, "Removal of Fe (III), Cu (II), and Co(II) from aqueous solutions by orange peels powder: equilibrium study," *Journal of Biochemistry and Molecular Biology Research*, vol. 2, no. 6, pp. 46–51, 2017.

[18] B. Hania and S. H. Alhaj, "Removal of cadmium(II) ION from aqueous solutions by orange peel," *GSJ*, vol. 7, no. 2, 2019.

[19] M. M. El-Ajaily, H. B. Alhaj, A. A. Erdeni, T. H. Al-Noor, and S. H. Al-Mabrouk, "Removal of Cadmium(II) ion from aqueous solutions by the outer layer of Onion," *IOP Conference Series: Earth and Environmental Science*, vol. 790, no. 1, Article ID 12011, 2021.

[20] S. M. Shartooh, S. A. Kasim, R. H. Obaid, A. A. Hadi, and A. A. Abdulmajeed, "Lettuce leaves as biosorbent material to remove heavy metal ions from industerial wastewater," *Baghdad Science Journal*, vol. 11, no. 3, pp. 1164–1170, 2014.